P	pressure, Pa
P_m	mixture pressure, Pa
ΔP	pressure change on mixing, Pa
R	molar gas constant, 8.314 41 J K^{-1} mol^{-1}
T	thermodynamic temperature, K
y	mole fraction

Appendix I. Effect of Component Impurity on B_{12}

If we label the primary components 1 and 2, consider an impurity in 1 labeled 6, and use the truncated pressure series virial equation, we obtain the following.

$$V = (RT/P + B_{m1})(n_1 + n_6) \qquad (A1)$$

$$V = (RT/P + B_{22})n_2 \qquad (A2)$$

$$2V = (RT/P_m + B_m)(n_1 + n_2 + n_6) \qquad (A3)$$

Equating (A3) with (A1) + (A2) and dividing by $(n_1 + n_2 + n_6)$, we obtain

$$RT(1/P - 1/P_m) = B_m - (y_1 + y_6)\, B_{m1} - y_2B_{22} \qquad (A4)$$

Substituting $B_m = \sum_i \sum_j y_i y_j B_{ij}$, we obtain

$$RT(1/P - 1/P_m) = y_1^2B_{11} + y_2^2B_{22} + y_6^2B_{66} + 2y_1y_2B_{12} + 2y_1y_6B_{16} + 2y_2y_6B_{26} - y_1^2B_{11}/(y_1 + y_6) - y_6^2B_{66}/(y_1 + y_6) - 2y_1y_6B_{16}/(y_1 + y_6) - y_2B_{22} \qquad (A5)$$

Since y_6 is much smaller than y_1, the approximation $1/(1 + y_6/y_1) \simeq 1 - y_6/y_1$ is a good one, especially for the purposes of error estimation. With this substitution, collecting coefficients gives

$$RT(1/P - 1/P_m) = 2y_1y_2[B_{12} - 0.5(B_{11} + B_{22})] - B_{11}y_6(y_1 - 1) - B_{22}y_6y_2 + 2B_{16}y_6(y_1 - 1 + y_6/y_1) + 2B_{26}y_6y_2 + B_{66}y_6(y_6 - y_6/y_1 + y_6^2/y_1^2) \qquad (A6)$$

This expression may be used to calculate $B_{12} - 0.5(B_{11} + B_{22})$ or alternatively to assess possible uncertainties.

Now

$$B^E_{12} = B_{12} - 0.5(B_{11} + B_{22})$$

and

$$B^E_{12}(\text{apparent}) = RT(1/P - 1/P_m)/2y_1y_2$$

To assess the likely magnitude of the error associated with ignoring the effect of the impurity, we may assume $y_1 = y_2 = 0.5$ and ignore terms containing y_6^2. This gives

$$B^E_{12}(\text{apparent}) = B^E_{12} + y_6[B_{11} - B_{22} + 2B_{26} - 2B_{16}]$$

The extension to the case of more than one impurity is straightforward.

Literature Cited

(1) Jaeschke, M.; Audibert, S.; van Caneghem, P.; Humphreys, A. E.; Jassen-van Rosmalen, R.; Pellei, Q.; Michels, J. P. J.; Schouten, J. A.; ten Seldom, C. A. *High Accuracy Compressibility Factor Calculation for Natural Gases and Similar Mixtures by Use of a Truncated Virial Equation*. GERG Technical Monograph; GERG: 1988; p 2.
(2) McElroy, P. J.; Shannon, T. W.; Williamson, A. G. *J. Chem. Thermodyn.* **1980**, *12*, 371.
(3) Holste, J. C.; Young, J. G.; Eubank, P. T.; Hall, K. R. *AIChE J.* **1982**, *28*, 807.
(4) Kleinrahm, R.; Duschek, W.; Wagner, W.; Jaeschke, M. *J. Chem. Thermodyn.* **1988**, *20*, 621.
(5) Goodwin, R. D.; Roder, H. M.; Straty, G. C. *NBS Tech. Note* **1978**, 684.
(6) Goodwin, R. D. *Natl. Bur. Stand.*, [*Tech. Rep.*] *NBSIR* (*U.S.*) **1977**, 77.
(7) Thomas, R. H. P.; Harrison, R. H. *J. Chem. Eng. Data* **1982**, *27*, 1.
(8) McGlashan, M. L.; Potter, D. J. B. *Proc. R. Soc. London* **1982**, *A267*, 478.
(9) Zaalishvili, Sh. D. *Zh. Fiz. Khim.* **1956**, *30*, 1891.
(10) Martin, M. L.; Tremgrove, R. D.; Harris, K. R.; Dunlop, P. J. *Aust. J. Chem.* **1982**, *35*, 1525.
(11) Zaalishvili, Sh. D. *Zh. Fiz. Khim.* **1952**, *26*, 970.
(12) Gunn, R. D. Volumetric Properties of Non-Polar Gas Mixtures. M.S. Dissertation, University of California, Berkeley, 1958.
(13) Tsonopoulos, C. *AIChE J.* **1974**, *20*, 263.
(14) Hayden, J. G.; O'Connell, J. P. *Ind. Eng. Chem. Process Des. Dev.* **1975**, *14*, 209.
(15) Melvin, A.; Caluwaerts, J.; van Canegham, P.; Humphreys, A. E.; Jaeschke, M.; Jolibois, J.; Joosten, G. E. H.; Polgatti, G.; van Wezel, J. N. *Proceedings of the International Gas Research Conference*, 1986; Cramer, T. L., International Gas Research Conference: Rockville, MD, 1987; pp 144–1153.
(16) Chueh, P. L.; Prausnitz, J. M. *Ind. Eng. Chem. Fundam.* **1967**, *6*, 492.
(17) Prausnitz, J.; Anderson, T.; Grens, E.; Eckert, C.; Hseih, R.; O'Connell, J. *Computer Calculations for Multi-Component Vapour-Liquid and Liquid-Liquid Equilibria*; Prentice-Hall: Englewood Cliffs, NJ, 1980; p 149.
(18) Cowan, P.; McElroy, P. J.; Humphreys, A. E. British Gas PLC. London Research Station Report No. LRST927; London Research Station: London, Jan 1988.
(19) Barber, J. R.; Kay, W. B.; Teja, A. S. *AIChE J.* **1982**, *28*, 134.
(20) Bougard, J.; Jadot, R. *J. Chim. Phys., Phys. Chim. Biol.* **1976**, *73*, 415.

Received for review September 12, 1989. Revised March 12, 1990. Accepted March 26, 1990.

Heat Capacities of the Water–Lithium Bromide–Lithium Iodide System

Shigeki Iyoki,* Sanae Ohmori, and Tadashi Uemura

Department of Chemical Engineering, Faculty of Engineering, Kansai University, Suita, Osaka 564, Japan

The heat capacities of the water–lithium bromide–lithium iodide system (salt mole ratios 4:1) were measured in the range of temperatures from 283.15 to 343.15 K and in the range of absorbent concentrations from 15.4 to 66.6 wt %. An empirical formula for this system was obtained from the experimental data by the least-squares method. Maximum and average absolute deviations between the experimental data and the calculated values from this empirical formula were 0.95% and 0.33%, respectively. The heat capacity data obtained for this system were compared with the predicted values on the basis of the principle of a corresponding state proposed by Kamoshida et al.

Introduction

The water–lithium bromide system (*1*) is being used as the working fluid in absorption refrigerating machines, absorption heat pumps, and absorption heat transformers. The water–lithium bromide–lithium iodide system (salt mole ratios 4:1) was proposed in order to improve the performance characteristics of the water–lithium bromide system.

The heat capacity data for working medium–absorbent systems are one of the most important basic properties for the research and the design of absorption refrigerating machines, absorption heat pumps, and absorption heat transformers. This investigation was undertaken to obtain data on the heat capacities of lithium bromide–lithium iodide aqueous solutions in

0021-9568/90/1735-0317$02.50/0

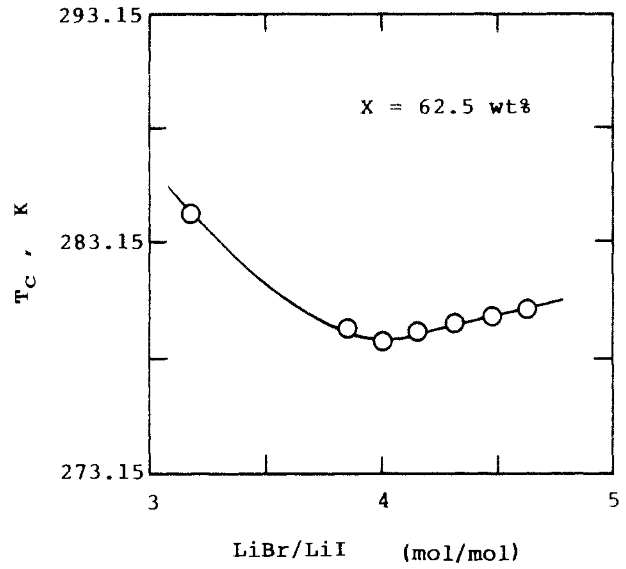

Figure 1. Relationship between mixing ratio and crystallization temperature.

the range of temperatures from 283.15 to 343.15 K and in the range of absorbent concentrations from 15.4 to 66.6 wt %. An empirical formula for the heat capacity of this system was obtained from the experimental data. The heat capacity data obtained for this system were compared with predicted values on the basis of the principle of a corresponding state proposed by Kamoshida et al. (*2*).

Experimental Section

Materials. The lithium bromide and lithium iodide used in this work were from the Honjo Chemical Co., Ltd. (Japan), analytical reagent grade. The analytical results of the lithium bromide aqueous solution were as follows: concentration, 55.0 wt %; Ca, 0.0002 wt %; Mg, 0.00002 wt %; Cl, 0.01 wt %; SO_4, 0.01 wt %. The analytical results of the lithium iodide aqueous solution were as follows: concentration, 56.2 wt %; Ca, 0.0023 wt %; Fe, 0.0001 wt %; SO_4, 0.012 wt %. All the reagents were used without further purification. The absorbent concentrations of the lithium bromide–lithium iodide aqueous solutions were determined by Fajans' method (*3*) with use of dichlorofluorescein as an adsorption indicator. The solution was titrated by using a microburette of 10-mL total delivery, with divisions of 0.02 mL.

The optimum mixing ratio of lithium bromide and lithium iodide was determined by measuring the crystallization temperature of sample solutions at constant absorbent concentration (62.5 wt %). Crystallization temperatures were obtained by changing the mixing ratio of lithium bromide in 1 mol of lithium iodide aqueous solutions. The constant-temperature bath was maintained to within ±0.01 K. The temperature was measured with a standard thermometer. Crystallization temperatures for various mixing ratios are shown in Figure 1. Consequently, the most suitable mixing ratio of lithium bromide and lithium iodide was found to be 4 and 1 mol, respectively.

Apparatus and Procedure. The heat capacities of lithium bromide–lithium iodide aqueous solutions were measured with a twin isoperibol calorimeter (Tokyo Riko Co., Ltd., Model TIC-22I). The accuracy of this apparatus was ±0.1%. The schematic diagram of the experimental apparatus used for heat capacity measurements is shown in Figure 2. The twin isoperibol calorimeter consisted of two Dewar vessels of the same size in a constant-temperature bath made of an aluminum block. The Dewar vessel was made of Pyrex glass. Each Dewar vessel was equipped with a heater, a thermistor, and a stirrer paddle. The Dewar vessel was sealed with a Teflon O ring. An accurately weighed sample solution and pure water (100 cm^3) were placed in each Dewar vessel. A magnetic stirrer was rotated by a synchronous motor at 140 rpm. The power supply was set at 50 mW. The heater was made of manganin wire, and the electric resistance of the heater was 100 Ω. After thermal equilibrium of both Dewar vessels was reached, electric current was passed for exactly 600 s to the heater. Dewar vessel temperature was measured with a thermistor. The temperature rises were recorded by a two-pen-type recorder. The heat capacities of the sample solutions were then calculated from eq 1, where Q is the energy input

$$Q = (mC + W)\Delta T \qquad (1)$$

(kJ), C is the heat capacity (kJ kg^{-1} K^{-1}), W is the thermal capacity (kJ K^{-1}) of the Dewar vessel determined from measurements using pure water (*4*) of known heat capacity, m is the weight (kg) of sample solution, and ΔT is the temperature rise (K). To check the accuracy of the apparatus and procedure, the heat capacities of p-xylene were measured at 298.15, 313.15, 333.15, and 343.15 K. The results are compared with those of other investigators (*5–7*) in Figure 3. The values obtained in this work agreed well with the results of Huffman et al. (*5*) and Corruccini et al. (*7*) with an average absolute deviation of less than 0.5%.

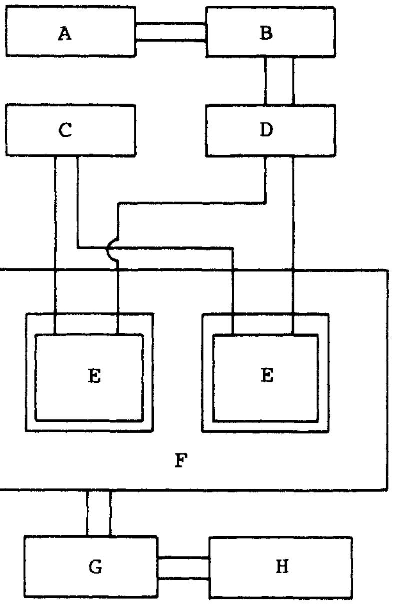

Figure 2. Experimental apparatus for measurements of heat capacity: A, recorder; B, integrator; C, power supply; D, amplifier; E, Dewar vessel; F, constant-temperature bath; G, volt adjustment unit; H, temperature controller.

Results and Discussion

The heat capacity data obtained in this work give C_p. The heat capacities of this system were measured in the range of temperatures from 283.15 to 343.15 K and in the range of absorbent concentrations from 15.4 to 66.6 wt %. The experimental results of 32 measurements for this system at various temperatures and absorbent concentrations are shown in Table I along with heat capacity values calculated by the empirical formula given in eq 2. The experimental results were

$$C_p = \sum_{n=0}^{4} A_n X^n + T\sum_{n=0}^{4} B_n X^n + T^2\sum_{n=0}^{4} C_n X^n \qquad (2)$$

plotted in Figure 4 as heat capacity at constant pressure. In this figure, the solid lines indicate the calculated values from the

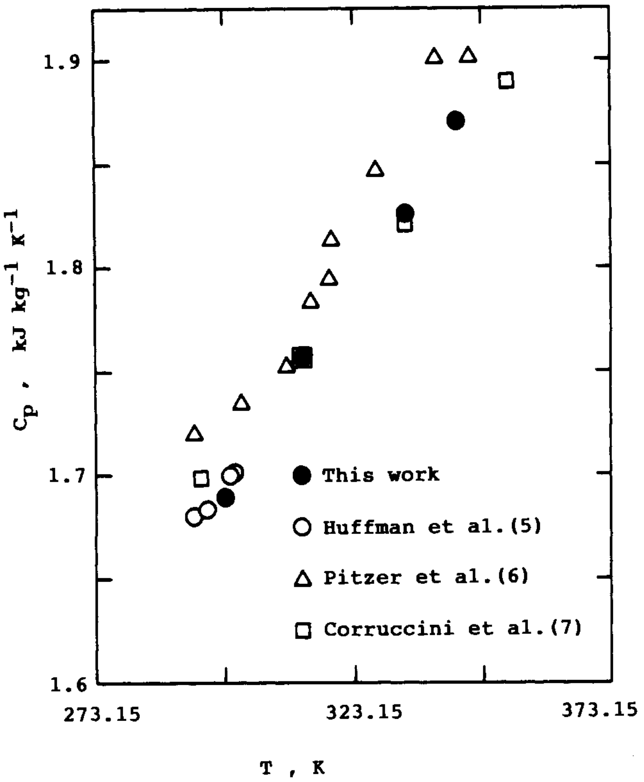

Figure 3. Heat capacities of *p*-xylene at various temperatures.

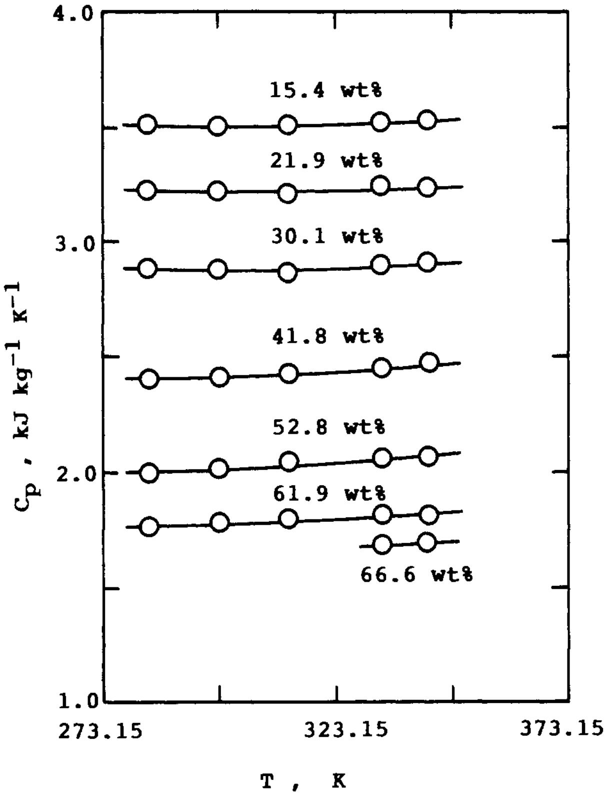

Figure 4. Heat capacities of H_2O–LiBr–LiI system (LiBr:LiI = 4:1 mol).

Table I. Heat Capacities of H_2O–LiBr–LiI System (LiBr:LiI = 4:1 mol)

T, K	$C_{p_{exp}}$, kJ kg^{-1} K^{-1}	$C_{p_{cal}}$, kJ kg^{-1} K^{-1}	ϵ, %
X = 15.4 wt %			
283.15	3.518	3.513	0.14
298.15	3.508	3.510	−0.06
313.15	3.518	3.511	0.20
333.15	3.521	3.521	0
343.15	3.531	3.528	0.08
X = 21.9 wt %			
283.15	3.227	3.222	0.15
298.15	3.222	3.223	−0.03
313.15	3.210	3.227	−0.53
333.15	3.244	3.239	0.15
343.15	3.237	3.248	−0.34
X = 30.1 wt %			
283.15	2.883	2.865	0.62
298.15	2.879	2.871	0.28
313.15	2.860	2.879	−0.66
333.15	2.902	2.895	0.24
343.15	2.909	2.905	0.14
X = 41.8 wt %			
283.15	2.404	2.399	0.21
298.15	2.415	2.410	0.21
313.15	2.429	2.423	0.25
333.15	2.448	2.444	0.16
343.15	2.474	2.455	0.77
X = 52.8 wt %			
283.15	2.005	2.024	−0.95
298.15	2.023	2.038	−0.74
313.15	2.054	2.054	0
333.15	2.062	2.076	−0.68
343.15	2.074	2.088	−0.68
X = 61.9 wt %			
283.15	1.772	1.765	0.40
298.15	1.784	1.780	0.22
313.15	1.805	1.795	0.55
333.15	1.823	1.816	0.38
343.15	1.820	1.827	−0.38
X = 66.6 wt %			
333.15	1.696	1.697	−0.06
343.15	1.703	1.707	−0.23

Table II. Values of A_n, B_n, and C_n in Empirical Formula 2

n	A_n	B_n	C_n
0	5.505 36	$-8.570\,79 \times 10^{-3}$	$1.370\,86 \times 10^{-5}$
1	$-5.866\,77 \times 10^{-2}$	$1.198\,91 \times 10^{-4}$	$-1.891\,41 \times 10^{-7}$
2	$-1.000\,96 \times 10^{-3}$	$3.361\,32 \times 10^{-6}$	$-3.415\,22 \times 10^{-9}$
3	$2.064\,89 \times 10^{-5}$	$-6.616\,76 \times 10^{-8}$	$7.269\,74 \times 10^{-11}$
4	$-9.018\,09 \times 10^{-8}$	$2.795\,97 \times 10^{-10}$	$-3.230\,37 \times 10^{-13}$

Table III. Comparison of Heat Capacities for the H_2O–LiBr–LiI System at 283.15 K

X, wt %	$C_{p_{exp}}$, kJ kg^{-1} K^{-1}	$C_{p_{pre}}$, kJ kg^{-1} K^{-1}	ϵ, %
15.4	3.518	3.782	−6.98
21.9	3.227	3.616	−10.76
30.1	2.883	3.415	−15.58
41.8	2.404	3.142	−23.49
52.8	2.005	2.895	−30.74
61.9	1.772	2.690	−34.13

empirical formula of eq 2. These experimental results were used to determine the constants for an empirical formula with a least-squares method. On the basis of the experimental data, the empirical formula (2) for the heat capacities of this system was obtained, where C_p is the heat capacity (kJ kg^{-1} K^{-1}) at constant pressure, T is the absolute temperature (K), and X is absorbent concentration (wt %) of aqueous solution. Values of the constants A_n, B_n, and C_n in empirical formula 2 are shown in Table II. Maximum and average absolute deviations between the experimental data and the calculated values from empirical formula 2 were 0.95% and 0.33%, respectively.

Moreover, the experimental data for this system at 283.15 K were compared with the predicted values on the basis of the principle of a corresponding state proposed by Kamoshida et al. (*2*). An unsaturated solution was dealt with an isothermal mixture of pure water and a saturated solution. The results are shown in Table III. The deviations between the experimental data and the predicted values were large, especially at high absorbent concentrations. Therefore, without using the predicted values on the basis of the principle of a corresponding state, it is necessary to measure heat capacity for this system.

Conclusions

The heat capacities of the three-component system using water as the working medium and lithium bromide–lithium iodide as the absorbent were measured at various temperatures and absorbent concentrations. An empirical formula for the heat capacity of this system was obtained by the least-squares method from the experimental data. The calculated values from this empirical formula were in good agreement with the experimental data. The heat capacity data of this system are very useful for the research and the design of absorption refrigerating machines, absorption heat pumps, and absorption heat transformers.

Glossary

A_n, B_n, C_n	constants in empirical formula 2
C_p	heat capacity at constant pressure, kJ kg^{-1} K^{-1}
n	integer exponent in empirical formula 2
T	absolute temperature, K
T_c	crystallization temperature, K
X	absorbent concentration, wt %

Greek Letter

ϵ	deviation, %

Subscripts

cal	calculated value from empirical formula 2
exp	experimental data
pre	predicted value on the basis of the principle of a corresponding state proposed by Kamoshida et al.

Literature Cited

(1) Uemura, T.; Hasaba, S. *Technol. Rep. Kansai Univ.* **1964**, *6*, 31–55.
(2) Kamoshida, J.; Hirata, H.; Isshiki, N.; Katayama, K.; Enomoto, E. Proceedings of the 23rd Japanese Joint Conference on Air-conditioning and Refrigeration, Tokyo, 1989; pp 77–80.
(3) Takagi, S. *Teiryo Bunseki no Jikken to Keisan*; Kyoritsu Shuppan: Tokyo, 1976.
(4) The Chemical Society of Japan. *Handbook of Chemistry*; Maruzen: Tokyo, 1984.
(5) Huffman, H. M.; Parks, G. S.; Daniels, A. C. *J. Am. Chem. Soc.* **1930**, *52*, 1547–1558.
(6) Pitzer, K. S.; Scott, D. W. *J. Am. Chem. Soc.* **1943**, *65*, 803–811.
(7) Corruccini, R. J.; Ginnings, D. C. *J. Am. Chem. Soc.* **1947**, *69*, 2291–2294.

Received for review October 6, 1989. Accepted May 1, 1990. We gratefully acknowledge the support for this research by the Yazaki Memorial Foundation for Science and Technology.

The Water Content of a CO_2-Rich Gas Mixture Containing 5.31 mol % Methane along the Three-Phase and Supercritical Conditions

Kyoo Y. Song and Riki Kobayashi*

Department of Chemical Engineering, George R. Brown School of Engineering, Rice University, P.O. Box 1892, Houston, Texas 77251

The water content of a carbon dioxide (CO_2)-rich phase containing 5.31 mol % methane (CH_4) and balance CO_2 in equilibrium with a water-rich phase was measured above the initial hydrate formation conditions and at isobars of 6.21, 7.59, 10.34, and 13.79 MPa, or of 900, 1100, 1500, and 2000 psia, respectively, at temperatures ranging from 15.6 °C (60 °F) to 50.0 °C (122 °F). The measurements indicated that the presence of 5.31 mol % methane in CO_2 lowered the water content value by 20–30% from that of pure CO_2. The water content of the mixture is superimposed on the pure CO_2 data for comparison. The relevant water content data are presented in both tabular and graphical forms.

Introduction

Since most CO_2-rich gases are likely to contain nitrogen or light hydrocarbons even after purification, the effect of the diluents on the saturated water content should be known. Earlier corresponding states computations suggested that relatively small amounts of diluents (5 mol %) would lower the water content significantly. Experiments were, therefore, proposed to measure the water content of CO_2 "contaminated" with about 5 mol % methane.

The water content of the CO_2-rich fluid phases had been measured earlier by Wiebe and Gaddy (*1*) and more recently by Song and Kobayashi (*2*). The latter studies were conducted both in the nonhydrate and hydrate regions. The earlier studies indicated that the water content was extremely sensitive to fluid densities, particularly in the supercritical CO_2 region. Therefore, the experimental efforts were concentrated in this region of temperature and pressure.

Experimental Detail

The experimental apparatus is divided into two major parts. One is an equilibrium apparatus shown in Figure 1, and the other is an analytical section, line diagram shown in Figure 2, which detects the amount of water in the sample drawn from the equilibrium cell.

The equilibrium apparatus was initially used for the study of the methane–carbon dioxide system by Mraw et al. (*3*) and subsequently for numerous vapor–liquid equilibrium (VLE) studies. Shown are a visual cell and a magnetic pump to promote efficient mixing and rapid equilibration of the contents of the cell.

The cell with an internal volume of 100 cm^3 has four sampling ports plus a bottom port. The multiplicity of sampling ports facilitates the withdrawal of sample from each phase of interest without contamination. The sampling lines beyond the sampling ports are heated to a temperature high enough to prevent the

---

* To whom all correspondence should be addressed.

0021-9568/90/1735-0320$02.50/0 © 1990 American Chemical Society